Total Least Squares in-field Identification for MEMS-based Triaxial Accelerometers

Massimo Ducchi, Federico Zaccaria, Sébastien Briot, Edoardo Idá

▶ **To cite this version:**

Massimo Ducchi, Federico Zaccaria, Sébastien Briot, Edoardo Idá. Total Least Squares in-field Identification for MEMS-based Triaxial Accelerometers. 16th IFToMM World Congress, Nov 2023, Yokohama, Japan. hal-04143770

HAL Id: hal-04143770
https://hal.science/hal-04143770v1

Submitted on 30 Jun 2023

HAL is a multi-disciplinary open access archive for the deposit and dissemination of scientific research documents, whether they are published or not. The documents may come from teaching and research institutions in France or abroad, or from public or private research centers.

L'archive ouverte pluridisciplinaire **HAL**, est destinée au dépôt et à la diffusion de documents scientifiques de niveau recherche, publiés ou non, émanant des établissements d'enseignement et de recherche français ou étrangers, des laboratoires publics ou privés.

Total Least Squares in-field Identification for MEMS-based Triaxial Accelerometers

Massimo Duchi[1], Federico Zaccaria[1,3], Sébastien Briot[2], and Edoardo Ida'[1]

[1] DIN, University of Bologna, Bologna, Italy
{massimo.duchi@studio.unibo.it,federico.zaccaria3,edoardo.ida2}@unibo.it
[2] CNRS, Laboratoire des Sciences du Numérique de Nantes (LS2N), Nantes, France,
Sebastien.Briot@ls2n.fr
[3] École Centrale de Nantes, Laboratoire des Sciences du Numérique de Nantes (LS2N), Nantes, France

Abstract. Micro-electro-mechanical system-based (MEMS-based) triaxial accelerometers are fundamental components of Inertial Measurement Units, and their use is widespread across various fields, such as the entertainment industry, robotics, and navigation systems. Various applications require that the cost of the sensor is not too high, which makes MEMS-based sensors a sensible choice. Unfortunately, low-cost MEMS are affected by relevant systematic errors which are time and environmental-condition dependent and thus require frequent re-calibration. Thus, simple calibration or identification methods, that a non-expert user can perform in the field without requiring costly equipment, are of interest. In this paper, we present an in-field identification procedure for MEMS-based triaxial accelerometers based on the linear Total Least Squares method.

Keywords: MEMS, Accelerometers, in-field calibration, in-field identification, Total Least Squares

1 Introduction

Triaxial accelerometers are sensors capable of converting a physical acceleration input into a voltage output. The relationship between input and output can be described by a linear function, which allows to define a mathematical model for the sensor [8]. Along with triaxial gyroscopes, accelerometers are widely used as components of *Inertial Measurement Units* (IMUs). IMUs are employed in many applications where the position and attitude of a body need to be estimated: civilian navigation systems, medical applications, robotics, but also commercial portable devices like computers and smartphones [10].

In order to satisfy large-scale demand, low-cost sensors based on *micro-electro-mechanical systems (MEMS-based)* are preferred, since they are typically more affordable than optical ones. However, the technologies and processes used for low-cost MEMS fabrication produce sensors with uncertain model parameters, which the manufacturer only estimates on batches [8]. If manufacturer-provided parameters are used in the sensor model, slight to large measurement

errors can be expected; when these measurements are to be post processed (as in IMUs), the errors are possibly further propagated and amplified [1].

Sensor errors can be divided into two categories: *systematical* and *random* errors. Systematical ones can be minimized by calibrating the sensor model parameters; essentially, the best fit between the mathematical model output and a known reference is sought. Calibration techniques for MEMS-based accelerometers can be divided into *Laboratory* and *In-Field* ones. The formers require high-precision instruments, such as mechanical rotating tables, in order to provide a known physical reference for the mathematical model output [8], whereas the latter do not require precision instrumentation, but the sensor must be placed in several orientations according to a predefined logic [5]. In-Field calibration methods are preferred for the frequent re-calibration of MEMS-based accelerometers.

In-Field calibration methods assume that the Euclidean norm of the acceleration measured by the sensor ($\mathbf{a}_m$) is constant and equal to the gravitational one ($\mathbf{g}$), in static conditions. Most methods require measuring sensor outputs by placing the accelerometer in different orientations, and to minimize a cost function $G(\boldsymbol{\theta}) = \sum_{i=1}^{N}(\|\mathbf{g}\|_2^2 - \|\mathbf{a}_{m,i}(\boldsymbol{\theta})\|_2^2)^2$, where N is the number of different orientations used, $\|.\|_2$ the Euclidean norm of a vector, and $\boldsymbol{\theta}$ the array collecting the model parameters to be found; the problem is usually solved with *Non-Linear Least Squares (NL-LS)* methods [9,11]. These methods do not require placing the sensor in specific orientations, which enhances usability, but they suffer from two main drawbacks: (i) they are based on non-linear optimization algorithms and consequently require a tentative initial parameter array, and (ii) the calibration output could be poor depending on the random orientations chosen by the user. A pre-calibration aiming to determine a valid initial guess for the iterative method was proposed in [13], but such a solution is quite time-consuming.

Methods for linear and non-iterative in-field calibration, which do not require any previous knowledge of the parameters to be calibrated, can be classified as identification methods and are naturally desirable. They were proposed in [3,5], but they can only be used under strict assumptions, such as (i) a surface orthogonal to earth gravity is available, and (ii) sensor parameters are within known bounds. Other classes of identification methods [14,15,7] are based on a suitable non-linear change of variables in the sensor model, which allows reformulating the classical NL-LS of [9,11] into linear ones. On the other hand, once the coefficients are found, the inverse transformation of the non-linear change of variables needs to be performed, numerically propagating the errors in the estimated parameters.

In this paper, we propose an in-field identification method based on (i) a predetermined sequence of rotations, used to acquire sensor outputs, and (ii) the solution of a Total Least Squares (TLS) problem. The sensor is placed in a 3D-printed multifaceted housing which is rotated with respect to a sloped surface used as a reference. The TLS approach ensures that potential errors in the rotations are accounted for while calibrating. The rest of the paper is organized as follows: Sec. 2 presents the description of the identification algorithm, while

experiments on *ADXL335* sensor are presented in Sec. 3. Section 4 concludes the paper.

2 Identification Algorithm Descrtiption

The mathematical model of a triaxial accelerometer, which correlates the acceleration in a frame attached to the sensor $\mathbf{a}' \in \mathbb{R}_{3\times1}$ with the voltage signal generated by the sensor $\mathbf{v} = [v_x, v_y, v_z]^T$, is given by [8,10]:

$$\mathbf{v} = \mathbf{S}'\mathbf{a}' + \mathbf{b}' + \boldsymbol{\epsilon}' \tag{1}$$

where $\mathbf{S}' \in \mathbb{R}_{3\times3}$ is a scale factor matrix, $\mathbf{b}' \in \mathbb{R}_{3\times1}$ is a vector containing bias terms and $\boldsymbol{\epsilon}' \in \mathbb{R}_{3\times1}$ is an array containing measurement noise. Although this model can well represent the physical behavior of the accelerometer, its inverse model is more convenient for practical uses:

$$\mathbf{a}' = \mathbf{S}(\mathbf{v} + \boldsymbol{\epsilon}) + \mathbf{b} \tag{2}$$

where $\mathbf{S} = \mathbf{S}'^{-1}, \mathbf{b} = -\mathbf{S}'^{-1}\mathbf{b}', \boldsymbol{\epsilon} = -\boldsymbol{\epsilon}'$. The aim of sensor identification is to determine the elements of matrix $\mathbf{S}$ and vector $\mathbf{b}$, so that voltage measurements $\mathbf{v}$ can be transformed into accelerations $\mathbf{a}'$. We assume $\mathbf{S}$ to be symmetric, and noise terms to be white Gaussian with zero mean [8]. The diagonal terms of $\mathbf{S}$ are referred to as *sensitivities*, while the off-diagonal terms as *cross sensitivities*. Cross sensitivities are non-zero when the three sensing axes in the accelerometer are not perfectly orthogonal with each other, and allow to account for this type of non-ideality, which is frequent in low-cost sensors [10]. Under such hypotheses, the model relies on 9 unknown parameters.

The proposed identification method requires placing the sensor inside a multifaceted housing, and re-orient such housing *with respect to* (w.r.t.) a reference surface in a predefined order. Such a surface is, in general, sloped; that is, our method does not require the reference to have a known orientation w.r.t. earth gravity, which is the main shortcoming of known identification methods [3,5]. Let $Oxyz$ be a fixed coordinate system attached to the reference surface, with z being the direction normal to the reference, and $O'x'y'z'$ a mobile system, attached to the accelerometer's theoric triad. When the identification procedure starts, the sensor housing (and thus the mobile frame) is aligned with the fixed frame, namely $Oxyz \equiv O'x'y'z'$. If we assume earth gravity to have a constant magnitude equal to g, we can define the acceleration perceived by the sensor in the start configuration as:

$$\mathbf{a}'_s = g\mathbf{n}_s \tag{3}$$

where $\mathbf{n}_s = [n_{sx}, n_{sy}, n_{sz}]^T$ is a unit vector (i.e. its Euclidean norm is one) expressing earth gravity direction in the mobile frame. $\mathbf{n}_s$ is generally unknown since the orientation of the reference w.r.t. earth gravity is random, and it will be calculated as a subproduct of the identification problem. To calibrate the sensor, its voltage outputs for different orientations need to be acquired. If r

re-orientations of the sensor are performed, the i-th acceleration perceived by the sensor, with $i = 1, ..., r$ is:

$$\mathbf{a}'_i = \mathbf{R}_i \mathbf{a}'_s \tag{4}$$

where $\mathbf{R}_i$ is a rotation matrix defined by a sequence of rotations performed w.r.t. the fixed frame, which in practice is achieved by placing the sensor housing on each of its facets sequentially. If we substitute Eq. (4) into Eq. (2), we can correlate the measured voltage with the acceleration in the start configuration as:

$$\mathbf{a}'_i = \mathbf{R}_i \mathbf{a}'_s = \mathbf{S}(\mathbf{v}_i + \boldsymbol{\epsilon}_i) + \mathbf{b} \tag{5}$$

Since the noise is generally well-modeled as white, additive, and Gaussian, we can mitigate its effect in Eq. (5) by considering the average voltage $\bar{\mathbf{v}}_i$ over k consecutive measurements in the same orientation is considered, namely:

$$\bar{\mathbf{v}}_i = \frac{\sum_{j=1}^{k} (\mathbf{v}_{i,j} + \boldsymbol{\epsilon}_{i,j})}{k}, \qquad k \gg 1 \tag{6}$$

and, finally, the *noiseless* mathematical model is obtained as:

$$\mathbf{a}'_i = \mathbf{R}_i \mathbf{a}'_s = \mathbf{S}\bar{\mathbf{v}}_i + \mathbf{b} \tag{7}$$

Rearranging Eq. (7) so as to highlight known quantities and unknown parameters to be calibrated, yields:

$$\mathbf{M}_i \boldsymbol{\theta} = \mathbf{0}_{3\times 1} \tag{8}$$

where:

$$\mathbf{M}_i = \begin{bmatrix} \bar{v}_{ix} & \bar{v}_{iy} & \bar{v}_{iz} & 0 & 0 & 0 & 1 & 0 & 0 & -R_{i,11} & -R_{i,12} & -R_{i,13} \\ 0 & \bar{v}_{ix} & 0 & \bar{v}_{iy} & \bar{v}_{iz} & 0 & 0 & 1 & 0 & -R_{i,21} & -R_{i,22} & -R_{i,23} \\ 0 & 0 & \bar{v}_{ix} & 0 & \bar{v}_{iy} & \bar{v}_{iz} & 0 & 0 & 1 & -R_{i,31} & -R_{i,32} & -R_{i,33} \end{bmatrix} \tag{9}$$

$$\boldsymbol{\theta} = \begin{bmatrix} S_{11} & S_{12} & S_{13} & S_{22} & S_{23} & S_{33} & b_x & b_y & b_z & n_{sx} & n_{sy} & n_{sz} \end{bmatrix}^T \tag{10}$$

and $R_{i,uw}$ and S_{uw} are the elements in the u-th row and w-th column of $\mathbf{R}_i$ and $\mathbf{S}$ respectively. According to our identification method, the gravity direction in the start configuration $\mathbf{n}_s$, expressed in the mobile frame, is also unknown and included in the parameters to be determined. By stacking Eq. (8) for $i = 1, \ldots, r$ measurements, we obtain an homogeneous system of $3r$ linear equations in 12 unknowns, which is overdetermined if $r > 4$:

$$\begin{bmatrix} \mathbf{M}_1 \\ \vdots \\ \mathbf{M}_r \end{bmatrix} \boldsymbol{\theta} = \mathbf{M}\boldsymbol{\theta} = \mathbf{0}_{3r\times 1}, \mathbf{M} \in \mathbb{R}_{3r\times 12} \tag{11}$$

Equation (11) can be solved for $\boldsymbol{\theta}$ with the linear *TLS* method (see [12] for the theoretical foundations, or [6,4] for practical applications). Please note that $\boldsymbol{\theta}$ contains the actual parameters needed by the model, and not a combination of them, which is the second shortcoming of previous works [7,14,15]. In ideal conditions, namely, without any measurement noise or model error, $\mathbf{M}$ should

be full-column rank deficient, namely rank($\mathbf{M}$) < 12, and a solution to Eq. (11) different to the trivial one (which is $\boldsymbol{\theta} = \mathbf{0}$) could be found. In real applications, it is necessary to address a compatible system that is closest to Eq. (11) in terms of the Frobenious norm:

$$\hat{\mathbf{M}}\hat{\boldsymbol{\theta}} = \mathbf{0} \tag{12}$$

where $\hat{\boldsymbol{\theta}}$, which is the solution to Eq. (11), contains the unknown parameters estimations and $\hat{\mathbf{M}}$ has rank 11 and minimizes $\|\hat{\mathbf{M}} - \mathbf{M}\|_F$, where $\|.\|_F$ is the Frobenius norm. $\hat{\mathbf{M}}$ can be computed by means of the "economy size" *singular values decomposition* of $\mathbf{M}$, given by

$$\mathbf{M} = \mathbf{U} \begin{bmatrix} diag(\delta_l) \\ \mathbf{0} \end{bmatrix} \mathbf{V}^T \tag{13}$$

where $\mathbf{U} \in \mathbb{R}_{3r\times 3r}$ and $\mathbf{V} \in \mathbb{R}_{12\times 12}$ are orthonormal matrices and $diag(\delta_l) \in \mathbb{R}_{12\times 12}$ is a diagonal matrix containing the singular values δ_l, for $l = 1, \ldots, 12$ of $\mathbf{M}$ sorted in decreasing order. $\hat{\mathbf{M}}$ can be obtained as

$$\hat{\mathbf{M}} = \mathbf{M} - \delta_{12}\mathbf{U}_{12}\mathbf{V}_{12}^T \tag{14}$$

being δ_{12} the smallest singular value of $\mathbf{M}$, and $\mathbf{U}_{12}, \mathbf{V}_{12}$ the 12-th columns of $\mathbf{U}$ and $\mathbf{V}$, respectively. A solution to Eq. (12) is given by $\hat{\boldsymbol{\theta}} = \mathbf{V}_{12}$. The solution to the proposed identification problem is obtained by normalizing $\hat{\boldsymbol{\theta}}$ so that its last three elements have unitary Euclidean norm, namely:

$$\boldsymbol{\theta} = \frac{\hat{\boldsymbol{\theta}}}{\|\hat{\boldsymbol{\theta}}_{10:12}\|_2} \tag{15}$$

where $\hat{\boldsymbol{\theta}}_{10:12}$ is the array collecting the last three elements of $\hat{\boldsymbol{\theta}}$.

The accuracy of the obtained results can be inferred by estimating the percentage relative standard deviations of the identified parameters. The estimation is performed according to the TLS techniques, and by assuming n_{sz} as the element having the maximum accuracy. Accordingly, the covariance matrix of the TLS solution may be approximated as [12]:

$$C_\theta = \hat{\sigma}_M^2(1 + \|\boldsymbol{\theta}_{1:11}\|_2^2)(\hat{\mathbf{M}}_{1:11}^T\hat{\mathbf{M}}_{1:11})^{-1} \tag{16}$$

where $\hat{\sigma}_M$ is

$$\hat{\sigma}_M = \frac{\delta_{12}}{\sqrt{3r - 12}} \tag{17}$$

and $\hat{\mathbf{M}}_{1:11}$ is obtained by discarding the last column of $\hat{\mathbf{M}}$, whereas $\boldsymbol{\theta}_{1:11}$ is the array containing the first 11 elements of $\boldsymbol{\theta}$. We finally obtain the percentage relative standard deviation estimations as [4]:

$$\sigma_{\%,\theta_l} = 100\frac{\sqrt{\mathbf{C}_{\boldsymbol{\theta}}(l,l)}}{|\theta_l|}, \qquad l = 1, \ldots, 11 \tag{18}$$

where $\mathbf{C}_{\boldsymbol{\theta}}(l,l)$ is the l-th diagonal term of $\mathbf{C}_{\boldsymbol{\theta}}$ and θ_l the l-th element of $\boldsymbol{\theta}$.

Algorithm 1 Rotation matrices computation for parallelepiped housing

```
i = 0;
for α = 0, α+ = π/2, α ≤ 3/2 π do
    for γ = 0, γ+ = π/2, γ ≤ 3/2 π do
        i = i + 1;
        R_i = (R'_i(α, 0, γ))^T;
    end for
end for
for β = π/2, β+ = π, β ≤ 3/2 π do
    for γ = 0, γ+ = π/2, γ ≤ 3/2 π do
        i = i + 1;
        R_i = (R'_i(0, β, γ))^T;
    end for
end for
```

Algorithm 2 Rotation matrices computation for 18-Faced housing

```
i = 0;
for α = 0, α+ = π/4, α ≤ 7/4 π do
    if α ≠ π/2, 3/2 π then
        for γ = 0, γ+ = π/2, γ ≤ 3/2 π do
            i = i + 1;
            R_i = (R'_i(α, 0, γ))^T
        end for
    end if
end for
for β = 0, β+ = π/4, β ≤ 7/4 π do
    if β ≠ 0, π/2, π, 3/2 π then
        for γ = 0, γ+ = π/2, γ ≤ 3/2 π do
            i = i + 1;
            R_i = (R'_i(0, β, γ))^T
        end for
    end if
end for
for β = 0, β+ = π/4, β ≤ 7/4 π do
    for γ = 0, γ+ = π/2, γ ≤ 3/2 π do
        i = i + 1;
        R_i = (R'_i(π/2, β, γ))^T
    end for
end for
```

3 Experimental Results

The proposed method was tested by producing simple 3D-printed sensor housings (where the sensor was rigidly attached) and references. Such equipment consists of a regular rectangular prism sensor housing (Fig. 1a), an 18-faced sensor housing (Fig. 1b) (obtained by chamfering the edges of the former housing at 45°), a reference with three orthogonal surfaces and a base parallel to one of the surfaces (Fig. 1c), and a reference with three orthogonal surfaces, and a sloped base (Fig. 1d). A re-orientation scheme is defined for each housing. Since the sensor is rigidly attached to the housing, $\mathbf{R}_i$ matrices can be computed as rotations about fixed frame axes, consisting in placing the sensor housing in each possible orientation where three of its faces are in contact with the reference surfaces. Consequently, $r = 24$ and $r = 72$ orientations can be achieved with the prismatic and 18-faced housing, respectively.

It is important that the sequence of rotation is always the same, thus the sequence of rotations used in this paper are described in Algorithms 1 and 2, where $\mathbf{R}'_i(\alpha_i, \beta_i, \gamma_i) = \mathbf{R}_z(\gamma_i)\mathbf{R}_y(\beta_i)\mathbf{R}_x(\alpha_i)$, and $\mathbf{R}_x$, $\mathbf{R}_y$, $\mathbf{R}_z$ are elementary rotation matrices about x', y' and z' axis, respectively. Please note that $\mathbf{R}'_i(\alpha_i, \beta_i, \gamma_i)$ represents physical re-orientations, where the housing is first rotated about the fixed x axis, then about the y axis, and lastly about the z axis, and thus transforms a vector expressed in the moving frame into a vector expressed in the fixed frame. Since Eq. (7) requires the acceleration to be expressed in the moving frame, $\mathbf{R}_i = \mathbf{R}_i'^T$.

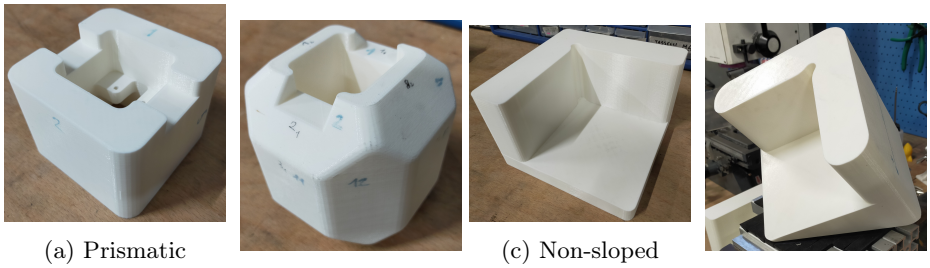

(a) Prismatic housing (b) 18-faced housing (c) Non-sloped reference (d) Sloped reference

Fig. 1: 3D-printed equipments

The re-orientation procedure is simpler for the prismatic housing since it has fewer faces. However, if a reference non-sloped w.r.t. $\mathbf{g}$ is used (e.g. the one in Fig. 1c), this re-orientation scheme is hardly optimal. In fact, if the reference rests on a surface reasonably orthogonal to $\mathbf{g}$, one of the sensor axes would be almost parallel to $\mathbf{g}$, and the others almost orthogonal: the measures obtained on each channel would be whether near the maximum possible or near zero, meaning that they would be characterized by high *noise-to-signal ratio* (NSR). To overcome this problem, one can: (i) use a sloped reference, so that all axes measurements have low NSR, or (ii) use a housing characterized by more possible orientations. Thus, experiments on all four possible combinations of references surface and housings were carried out. For each of the r configurations, we acquired $k = 1000$ samples at 1kHz from the three analog channels of an *Analog Devices ADXL335* accelerometer, using a 12-bit *Analog to Digital Converter* and a *STM32-L432KC Micro Controller Unit*.

Identification results are shown in Table 1. Elements of matrix $\mathbf{S}$ are expressed in [g/mV], while those of $\mathbf{b}$ and $\mathbf{n}_s$ are in [g], thus they are normalized with respect to the modulus of the gravitational acceleration. For the tested sensor, we obtained negligible values for off-diagonal elements of $\mathbf{S}$ w.r.t. diagonal ones, which means that the sensor's axes are well-aligned and there is no relevant cross-sensitivity effect between analog channels. Consequently, relative standard deviations associated with these parameters are really high (a parameter is considered well-identified if the percentage standard deviation is below 5%); namely, they are non-essential parameters for the specific sensor tested. Parameters identification best practice suggests excluding non-essential parameters from the model and performing a second identification with the simplified model, which does not include them [4]. Results for the identification of essential parameters are shown in Table 2. As we expected, experiments involving the 18-faced housing and the sloped reference gave the best results: in fact, they present the lowest relative standard deviation estimations among all the tests performed. However, we can say that, for each of the tests performed, all the essential parameters showed a small relative standard deviation estimation, less than the acceptability threshold of 5%, and are thus well identified.

θ_l	S_{11}	S_{12}	S_{13}	S_{22}	S_{23}	S_{33}	b_x	b_y	b_z	n_{sx}	n_{sy}
$\hat{\theta}_l$	2.89e-03	-2.91e-05	2.43e-06	2.91e-03	-3.94e-06	2.89e-03	-4.73	-4.75	-5.03	4.37e-03	1.56e-02
$\sigma_{\%,\theta_l}$	0.41	28.67	342.48	0.41	211.54	0.41	0.59	0.59	0.56	53.78	15.08

(a) Non-sloped reference, prismatic housing

θ_l	S_{11}	S_{12}	S_{13}	S_{22}	S_{23}	S_{33}	b_x	b_y	b_z	n_{sx}	n_{sy}
$\hat{\theta}_l$	2.89e-03	-3.04e-05	1.82e-06	2.91e-03	-4.96e-06	2.88e-03	-4.72	-4.74	-5.03	-3.90e-01	-4.91e-01
$\sigma_{\%,\theta_l}$	0.44	27.03	449.92	0.44	165.73	0.44	0.61	0.61	0.58	0.67	0.56

(b) Sloped reference, prismatic housing

θ_l	S_{11}	S_{12}	S_{13}	S_{22}	S_{23}	S_{33}	b_x	b_y	b_z	n_{sx}	n_{sy}
$\hat{\theta}_l$	2.89e-03	-3.04e-05	2.15e-06	2.90e-03	-5.32e-06	2.89e-03	-4.72	-4.73	-5.05	1.82e-02	8.51e-03
$\sigma_{\%,\theta_l}$	0.14	9.38	132.29	0.14	53.63	0.14	0.20	0.20	0.19	4.41	9.44

(c) Non-sloped reference, 18-faced housing

θ_l	S_{11}	S_{12}	S_{13}	S_{22}	S_{23}	S_{33}	b_x	b_y	b_z	n_{sx}	n_{sy}
$\hat{\theta}_l$	2.89e-03	-2.95e-05	3.31e-06	2.90e-03	-5.34e-06	2.88e-03	-4.73	-4.73	-5.05	-3.88e-01	-4.94e-01
$\sigma_{\%,\theta_l}$	0.16	10.01	89.00	0.16	55.19	0.16	0.22	0.22	0.21	0.24	0.20

(d) Sloped reference, 18-faced housing

Table 1: Results - Well-aligned sensor, all parameters

Finally, we cross-validated the identification results reported in Table 2d, by using the data sets acquired while performing the experiments relative to Tables 2a, 2b and 2c. For each data set, we computed $\mathbf{M}$ as in Eq. (9) and (11), and obtained the corresponding model error $\boldsymbol{\eta}$ as $\boldsymbol{\eta} = \mathbf{M}\boldsymbol{\theta}$. For the data sets involving the non-sloped reference, the last three elements of $\boldsymbol{\theta}$ were set $[0, 0, 1]^T$, while they were set to $[n_{sx}, n_{sy}, n_{sz}]^T$ for the data sets involving the sloped reference (n_{sz} is obtained by imposing $\|\mathbf{n}_s\|_2 = 1$, and n_{sx}, n_{sy} are in Table 2d).

Cross-validation standard deviations σ' are obtained as [6]:

$$\sigma' = \sqrt{\frac{\boldsymbol{\eta}^T\boldsymbol{\eta}}{3r}} \tag{19}$$

where $3r = 72$ for data sets with the prismatic housing and $3r = 216$ for the 18-faced ones. The worst-case standard deviation is $\sigma' = 0.0211g$. Additionally, we also evaluated a cross-validation standard deviation by using manufacturer-provided sensor parameters. Accelerometer's datasheet [2] only reports ranges of values for the sensor's model parameters so, without further information available, we adopted mean values of those ranges, i.e. sensitivities $S_{11} = S_{22} = S_{33} = \frac{1}{300}g/mV$, and biases $b_x = b_y = b_z = -5g$ according to the model of Eq. (2), with cross sensitivities equal to 1% of sensitivities. The best-case standard deviation, in this case, is $\sigma'_{=}0.525g$, which is 25 times the one obtained with the parameters identified by our method. It is thus clear that our method is a valid choice to improve accelerometers' accuracy at no relevant cost.

θ_l	S_{11}	S_{22}	S_{33}	b_x	b_y	b_z
$\hat{\theta}_l$	2.89e-03	2.91e-03	2.89e-03	-4.78	-4.80	-5.03
$\sigma_{\%,\theta_l}$	0.55	0.55	0.55	0.56	0.56	0.56

(a) Non-sloped reference, prismatic housing - essential parameters

θ_l	S_{11}	S_{22}	S_{33}	b_x	b_y	b_z	n_{sx}	n_{sy}
$\hat{\theta}_l$	2.89e-03	2.91e-03	2.88e-03	-4.77	-4.80	-5.04	-3.90e-01	-4.91e-01
$\sigma_{\%,\theta_l}$	0.48	0.48	0.48	0.49	0.49	0.49	0.73	0.61

(b) Sloped reference, prismatic housing - essential parameters

θ_l	S_{11}	S_{22}	S_{33}	b_x	b_y	b_z
$\hat{\theta}_l$	2.89e-03	2.90e-03	2.89e-03	-4.77	-4.79	-5.05
$\sigma_{\%,\theta_l}$	0.30	0.30	0.30	0.30	0.30	0.30

(c) Non-sloped reference, 18-faced housing - essential parameters

θ_l	S_{11}	S_{22}	S_{33}	b_x	b_y	b_z	n_{sx}	n_{sy}
$\hat{\theta}_l$	2.89e-03	2.90e-03	2.88e-03	-4.77	-4.78	-5.05	-3.88e-01	-4.94e-01
$\sigma_{\%,\theta_l}$	0.19	0.19	0.19	0.20	0.20	0.20	0.29	0.24

(d) Sloped reference, 18-faced housing - essential parameters

Table 2: Results - Well-aligned sensor, essential parameters

4 Conclusions

In this paper, we proposed an in-field identification procedure for MEMS-based accelerometers. Our method can be performed using simple 3D-printed equipment and without prior knowledge of the reference orientations w.r.t. $\mathbf{g}$, and requires performing a set of predefined re-orientation of the sensor, and the use of the linear TLS method. Experimental results showed that the sensor's model parameters can be correctly estimated by our method, and the accuracy of the sensor model is severely increased with respect to using manufacturer-provided model parameters. In the future, our method will be extended to gyroscope parameter identification, so as to provide a general identification method for IMUs.

References

1. Aggarwal, P., El-Sheimy, N., Noureldin, A., Syed, Z.: MEMS-Based Integrated Navigation. Artech (2010)
2. Analog Devices: Small, Low Power, 3-Axis ± 3g Accelerometer ADXL335 datasheet, `https://www.analog.com/media/en/technical-documentation/data-sheets/adxl335.pdf`

3. Forsberg, T., Grip, N., Sabourova, N.: Non-iterative calibration for accelerometers with three non-orthogonal axes, reliable measurement setups and simple supplementary equipment. Measurement Science and Technology 24(3), 035002 (feb 2013)
4. Gautier, M., Briot, S.: Global Identification of Joint Drive Gains and Dynamic Parameters of Robots. Journal of Dynamic Systems, Measurement, and Control 136(5) (07 2014), 051025
5. Grip, N., Sabourova, N.: Simple non-iterative calibration for triaxial accelerometers. Measurement Science and Technology 22(12), 125103 (oct 2011)
6. Idà, E., Briot, S., Carricato, M.: Identification of the inertial parameters of underactuated cable-driven parallel robots. Mechanism and Machine Theory 167, 104504 (2022)
7. Khankalantary, S., Ranjbaran, S., Ebadollahi, S.: Simplification of calibration of low-cost mems accelerometer and its temperature compensation without accurate laboratory equipment. Measurement Science and Technology 32(4), 045102 (feb 2021)
8. Poddar, S., Kumar, V., Kumar, A.: A Comprehensive Overview of Inertial Sensor Calibration Techniques. Journal of Dynamic Systems, Measurement, and Control 139(1) (09 2016), 011006
9. Qureshi, U., Golnaraghi, F.: An algorithm for the in-field calibration of a mems imu. IEEE Sensors Journal 17(22), 7479–7486 (2017)
10. Ru, X., Gu, N., Shang, H., Zhang, H.: Mems inertial sensor calibration technology: Current status and future trends. Micromachines 13(6) (2022)
11. Tedaldi, D., Pretto, A., Menegatti, E.: A robust and easy to implement method for imu calibration without external equipments. In: 2014 IEEE International Conference on Robotics and Automation (ICRA). pp. 3042–3049 (2014)
12. Van Huffel, S., Vandewalle, J.: The Total Least Squares Problem. Society for Industrial and Applied Mathematics (1991)
13. Won, S.h.P., Golnaraghi, F.: A triaxial accelerometer calibration method using a mathematical model. IEEE Transactions on Instrumentation and Measurement 59(8), 2144–2153 (2010)
14. Zhang, H., Wu, Y., Wu, M., Hu, X., Zha, Y.: A multi-position calibration algorithm for inertial measurement units. AIAA Guidance, Navigation and Control Conference and Exhibit (2008)
15. Zhang, H., Wu, Y., Wu, W., Wu, M., Hu, X.: Improved multi-position calibration for inertial measurement units. Measurement Science and Technology 21(1), 015107 (nov 2009)